Analysis of Time Information from 2006 BCAL Cosmics Runs

Andrei Semenov, George Lolos, Zisis Papandreou, and Irina Semenova
University of Regina

1 Data Set

This note describes an analysis of time information in four BCAL cosmics runs that were taken at Jefferson Lab in 2006: run 2458 (the trigger/paddle was positioned in +100 cm from the center of the calorimeter), run 2459 (+150 cm), run 2475 (-50 cm), and run 2476 (-150 cm). The correspondent *bcal_dst024##.root* files were taken from */work/halld/bcal06* directory.

2 Module Segmentation and Cosmic "Muon" Selection

The calorimeter module consists of 18 segments; the segments were arranged in vertical 6 columns (of 3 segments each); numbering of the segments is shown in Fig.1. Each of the segments 1-3, 7-9, and 13-15 was read out from both ends by two Philips XP2020 PMTs, while the read out of segments 4-6, 10-12, and 16-18 was done with Burle 8575 PMTs. After signal splitting, half of each of PMT signals was sent to CAEN V792 ADC, and another half was sent to leading-egde (a CAEN C207 equivalent) discriminator and further to JLab F1 TDC [1].

To select the cosmic "muon" (i.e., particle that is close to MIP) tracks in the certain segment in some of the columns, we require the high amplitude (viz., $adc > 70$) in the remaining segment of the column of interest as well as low amplitudes (viz., $adc < 10$) in all segments of the left neighbour and the right neighbour columns (see Fig.2). Such a criterion suppresses the events with a shower and picks out nearly vertical-oriented particle tracks in the calorimeter; it selects about 15-20% of the total number of events in the run. Each PMT signal amplitude in the selected data stream was corrected for ADC channel pedestal; the determination of pedestal values was done according to the procedure described in the note GlueX-doc-845.

3 Time-Walk Correction and Time Resolution

We analyze differences in the mean times for pair of segments in the same column (see Fig.3):

$$TOF(i,j) \;=\; [TDC_{North}(j) + TDC_{South}(j)]/2 \;-\; [TDC_{North}(i) + TDC_{South}(i)]/2 \;, \qquad (1)$$

where i and j are indexes of "Start" and "Stop" segments, accordingly; that procedure eliminates an influence of the start counter. Because leading-edge discriminators were used, the TOF value has a significant dependence on pulse amplitudes from all four participationg PMTs, and time-walk correction is needed. We fitted TOF-vs-ADC_i scatter plot to a function of the form

$$fit(ADC_i) \;=\; p_0 + p_1 \cdot (ADC_i)^{-1/2} + p_2 \cdot (ADC_i)^{-1/3} \;, \qquad (2)$$

and subtracted the fit from the TOF values; this correction procedure was repeated for each amplitude of four signals from the pair of segments. The resulting TOF_{corr} distribution is centered around zero and reflects a resolution of the timing between two BCAL segments of interest. An uncorrected TOF spectrum for segments 3 and 15 from run 2475, the consecutive time-walk corrections, and the final corrected spectrum are shown in Fig.4. Time resolution for each pair of segments in every column was extracted from fit of the TOF_{corr} spectrum to a gaussian distribution; the summaries of time resolutions from runs 2458, 2459, 2475, and 2476 are shown in Fig.5-8. For the pairs of segments that were read out using Philips XP2020 PMTs, the averaged over segment pairs time resolutions were (546±33) ps, (616±29) ps, (533±25) ps, and (683±23) ps for runs 2458, 2459, 2475, and 2476, accordingly.

For every column of the module, we have three segments with unknown intrinsic time resolutions, and we have three possible combinations of pairs of segments. Assuming that there is no correlation between time resolutions of segments in the pair, the time resolutions of pairs of segments in some column can be expressed via individual time resolutions of segments in the column (that gives us a system of three equations with three unknown parameters), and the time resolutions of individual segments can be extracted:

$$\left\{\begin{array}{lcl}\sigma_{ij}^2 &=& \sigma_i^2 + \sigma_j^2\\ \sigma_{ik}^2 &=& \sigma_i^2 + \sigma_k^2\\ \sigma_{jk}^2 &=& \sigma_j^2 + \sigma_k^2\end{array}\right. \quad => \quad \left\{\begin{array}{lcl}\sigma_i^2 &=& 0.5*(\sigma_{ij}^2 + \sigma_{ik}^2 - \sigma_{jk}^2)\\ \sigma_j^2 &=& 0.5*(\sigma_{ij}^2 + \sigma_{jk}^2 - \sigma_{ik}^2)\\ \sigma_k^2 &=& 0.5*(\sigma_{ik}^2 + \sigma_{jk}^2 - \sigma_{ij}^2)\,,\end{array}\right. \tag{3}$$

where i, j, and k are the indexes of the segments in the column. Time resolutions for each segment extracted from run 2458, 2459, 2475, and 2476 are shown in Fig.9-12. Distributions of segment time resolutions weighted on the uncertainty $\Delta\sigma_i$ of segment time resolution measurement:

$$Weight_i \sim \frac{1}{(\Delta\sigma_i)^2} \tag{4}$$

from four runs are shown in Fig.13.

4 Trigger Position Dependence

We assume that the time resolution of a single segment i for the muon hit in the center of the segment can be written in the form:

$$\sigma_i^2 = (\sigma_{iN}^2 + \sigma_{iS}^2)/4 = \frac{C^2}{N_{phe}} + B^2 = \frac{A^2}{\Delta E} + B^2\,, \tag{5}$$

where σ_{iN} and σ_{iS} are the time resolutions of the North and South PMTs of the segment, N_{phe} is the number of photoelectrons, and ΔE is the correspondent energy deposition in the segment fibers. The time resolution of a pair of segments for the muon hit in x cm from the centers of segments is expressed in the form:

$$\begin{array}{rcl}\sigma_{ij}^2 &=& (\sigma_{iN}^2 + \sigma_{iS}^2)/4 + (\sigma_{jN}^2 + \sigma_{jS}^2)/4 = \frac{C^2}{N_{phe}\cdot e^{x/L}} + B^2 + \frac{C^2}{N_{phe}\cdot e^{-x/L}} + B^2\\ &=& \frac{A^2}{\Delta E}(e^{x/L} + e^{-x/L}) + 2\cdot B^2\,,\end{array} \tag{6}$$

where L is the attenuation length of the light in the calorimeter module (we use the value L = 229.1 cm from the report GlueX-doc-845). In theory, using the time resolutions extracted from the runs with different positions of the trigger counters (viz., different positions of the

muon hits), we can try to separate the statistical (viz., energy-dependent) and floor terms. We simulated the energy deposition ΔE in the fibers (see Fig.14) from the muons in the realistic model of the calorimeter using FLUKA 2006.3b program [2,3] and fitted the time resolutions of the pair of segments (averaged over the segments that were read out with Philips XP2020 PMTs) to the function (5). We estimate the statistical term as $A = (28.5 \pm 1.7)$ ps, and the floor term as $B = (0.000002 \pm 211)$ ps [see Fig.15]. Projecting these results on the module test with a beam of photons and assuming the module sampling fraction (from the simulation with FLUKA) $\Delta E_{fiber}/\Delta E_{\gamma} = 0.129$, we can predict the time resolution of single segment as a function of photon energy:

$$\sigma \;=\; \frac{(79.3 \,\pm\, 4.7)\; ps}{\sqrt{E_{\gamma}(GeV)}} \;\oplus\; (0.000002 \,\pm\, 211)\; ps \tag{7}$$

The statistical term of the time resolution is in a good agreement with the value obtained from the analysis of photon beam test data [1]. Unfortunately, a limited set of cosmics trigger positions available and pure statistics of the cosmics data do not allow to make any certain conclusion about the floor term.

References

[1] B.D. Leverington et al. Nucl. Instrum. Meth. **A596**, 327 (2008).

[2] A. Fasso, A. Ferrari, P.R. Sala, Electron-Photon Transport in FLUKA: Status, Proceedings of the Monte Carlo 2000 Conference, Lisbon, October 23-26, 2000, A. Kling, F. Barao, M. Nakagawa, L. Tavora, P. Vaz eds., Springer-Verlag Berlin, pp. 159-164 (2001).

[3] A. Fasso, A. Ferrari, J. Ranft, P.R. Sala, FLUKA: Status and Perspective for Hadronic Applications, Proceedings of the Monte Carlo 2000 Conference, Lisbon, October 23-26, 2000, A. Kling, F. Barao, M. Nakagawa, L. Tavora, P. Vaz eds., Springer-Verlag Berlin, pp. 955-960 (2001).

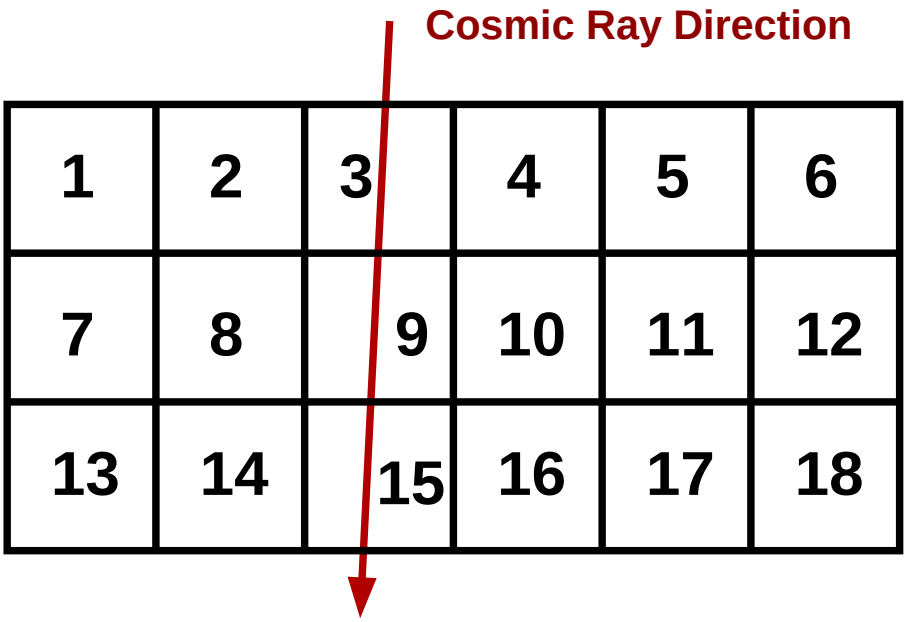

Figure 1: Numbering of BCAL segments in 2006 cosmics test at JLab (as viewed from its North end).

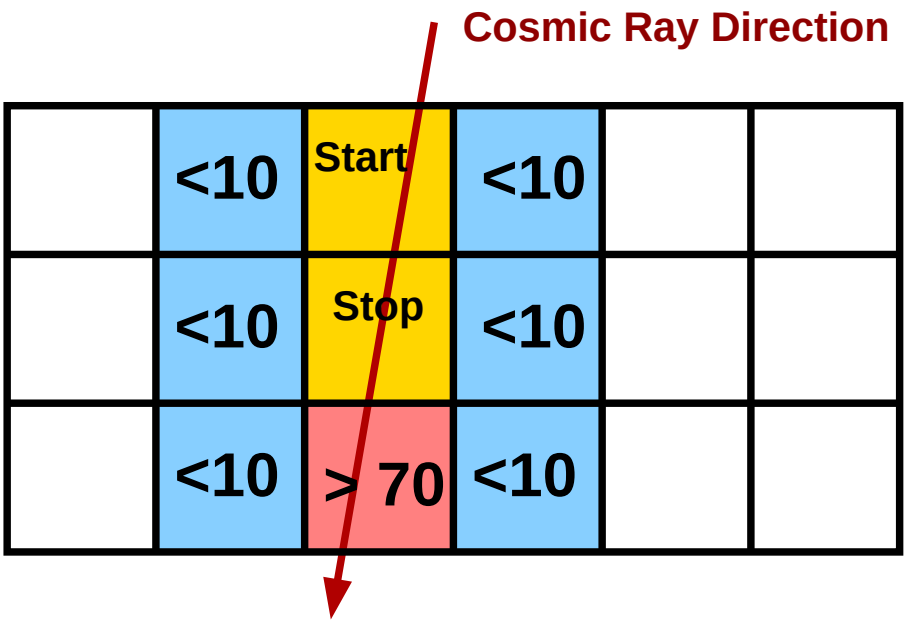

Figure 2: Selection of "muon" events in BCAL cosmics data.

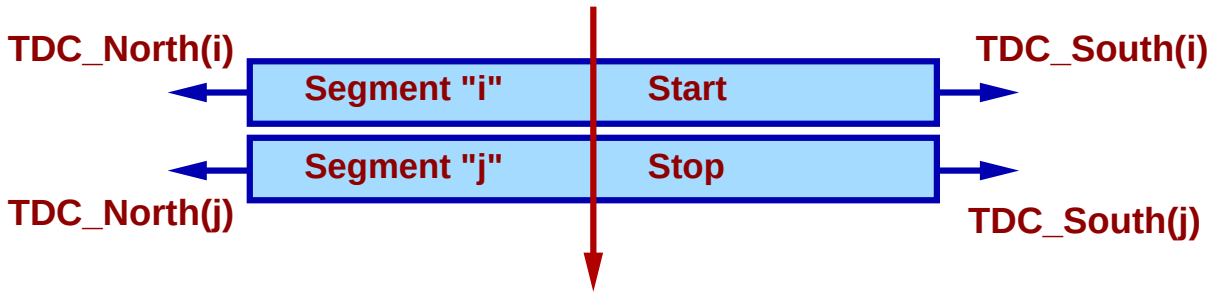

Figure 3: Difference in the mean times from two segments in the BCAL column.

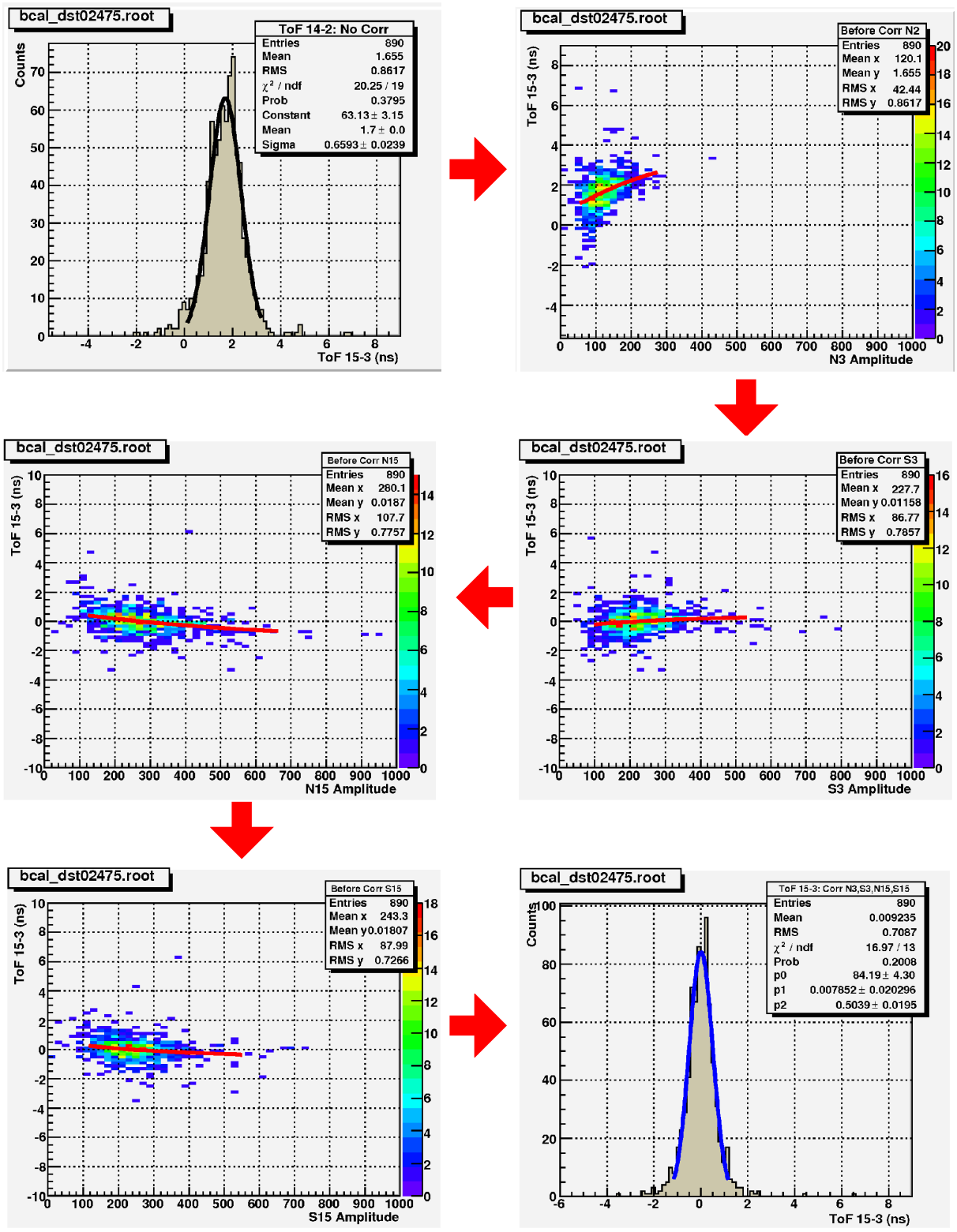

Figure 4: An uncorrected TOF spectrum ($\sigma = 660 \pm 24$ ps) for segments 3 and 15 from run 2475, the consecutive time-walk corrections, and the final corrected spectrum with a time resolution of (504±20) ps.

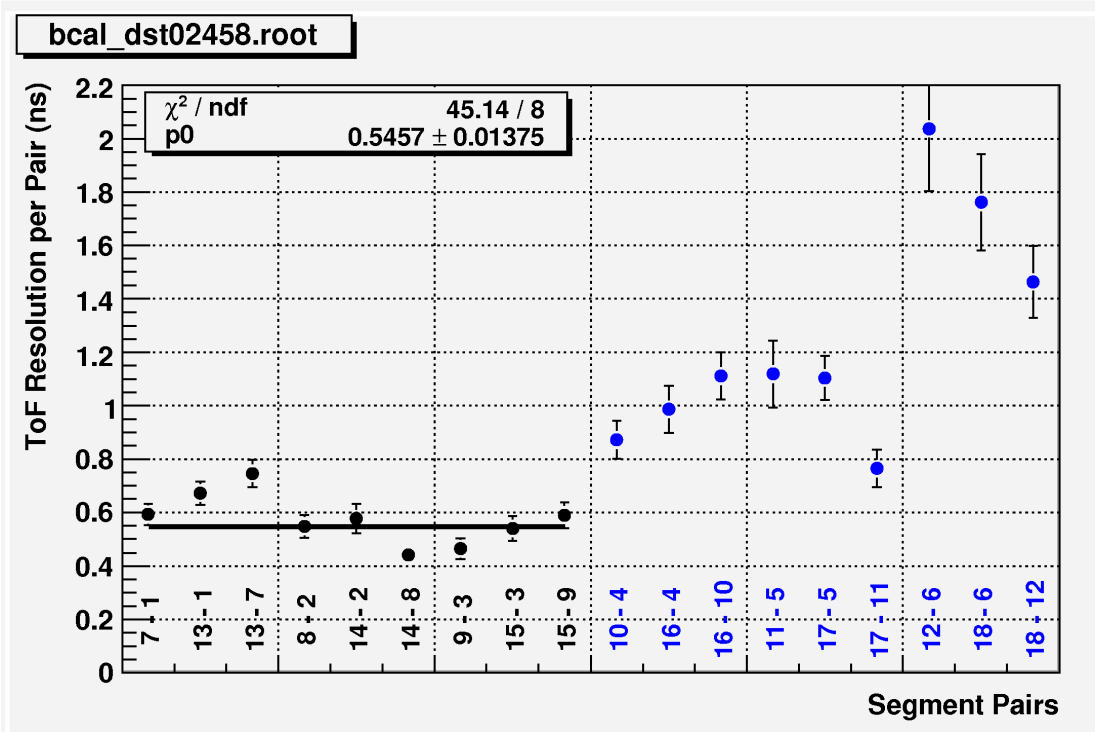

Figure 5: Summary of time resolutions from run 2458. For the pairs of segments that were read out using Philips XP2020 PMTs (black symbols), the averaged over segment pairs time resolution was (546±33) ps.

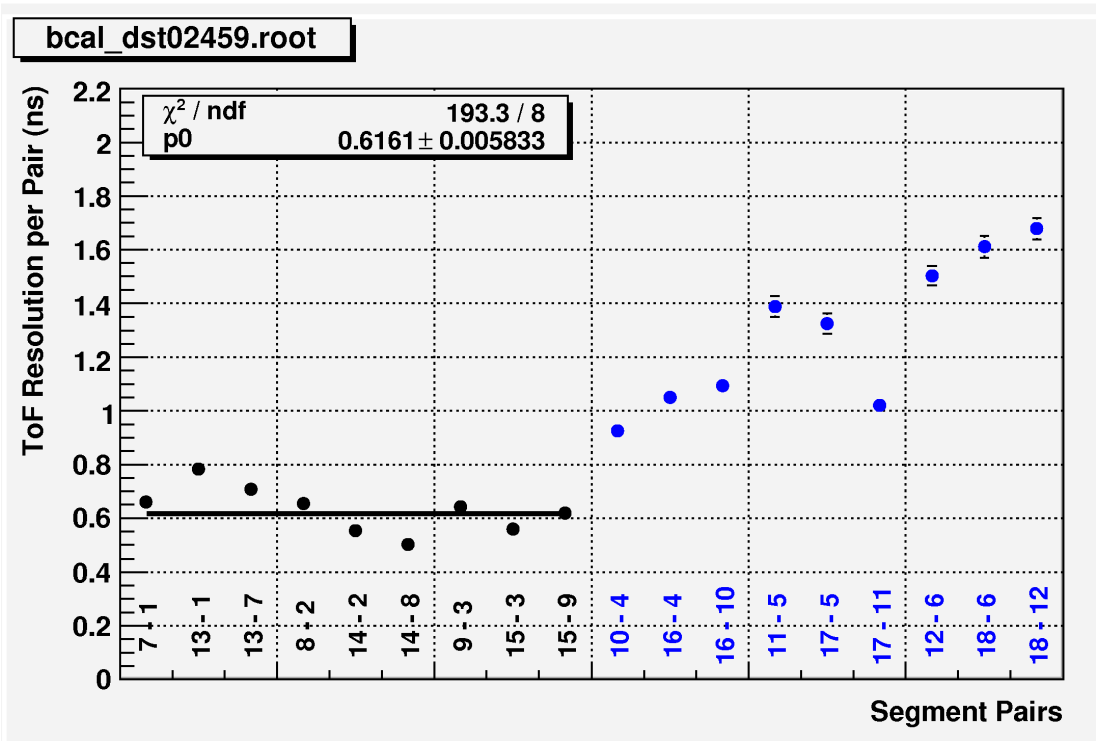

Figure 6: Summary of time resolutions from run 2459. For the pairs of segments that were read out using Philips XP2020 PMTs (black symbols), the averaged over segment pairs time resolution was (616±29) ps.

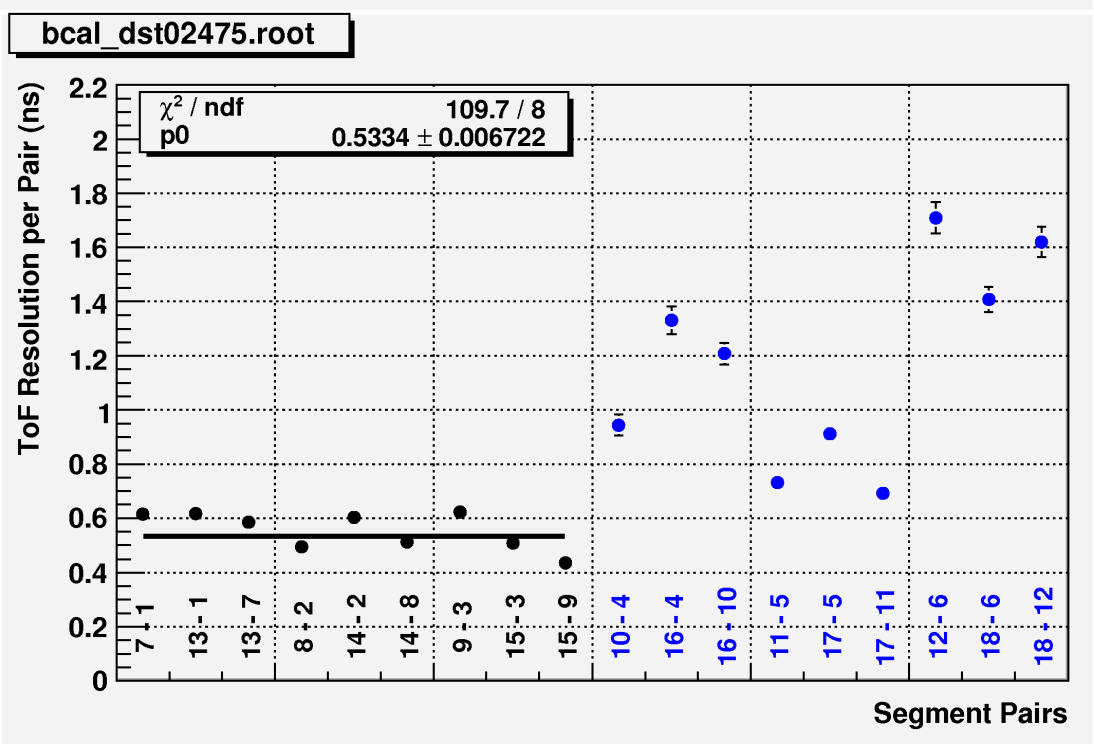

Figure 7: Summary of time resolutions from run 2475. For the pairs of segments that were read out using Philips XP2020 PMTs (black symbols), the averaged over segment pairs time resolution was (533±25) ps.

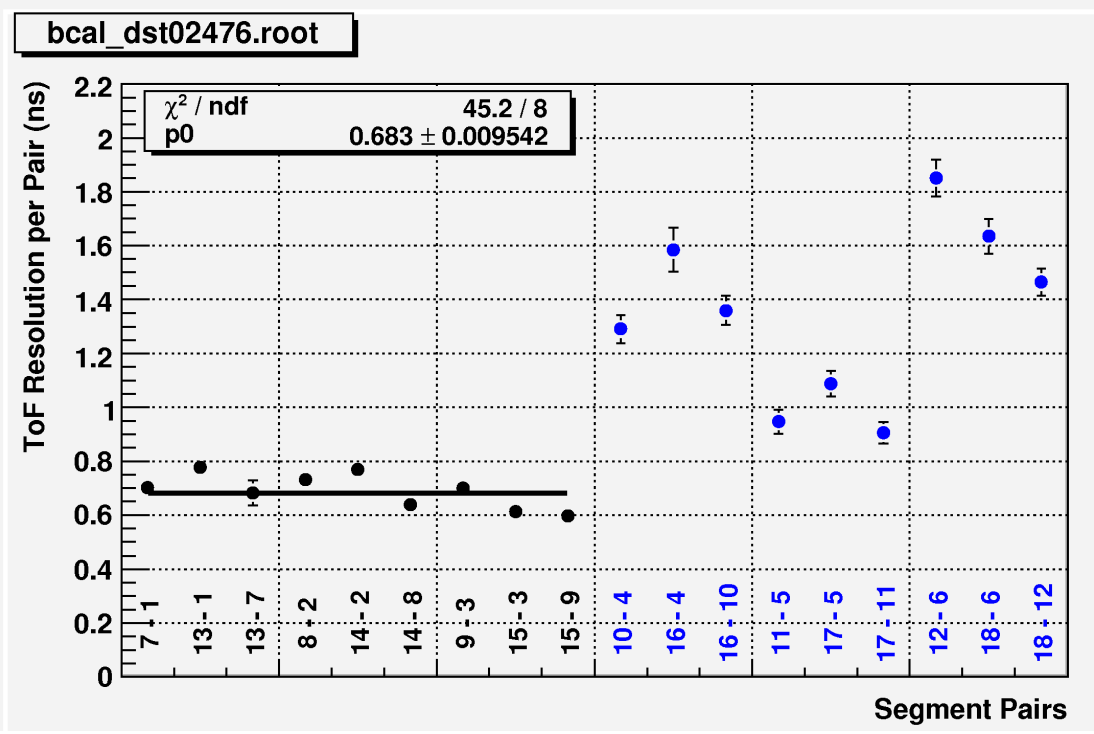

Figure 8: Summary of time resolutions from run 2476. For the pairs of segments that were read out using Philips XP2020 PMTs (black symbols), the averaged over segment pairs time resolution was (683±23) ps.

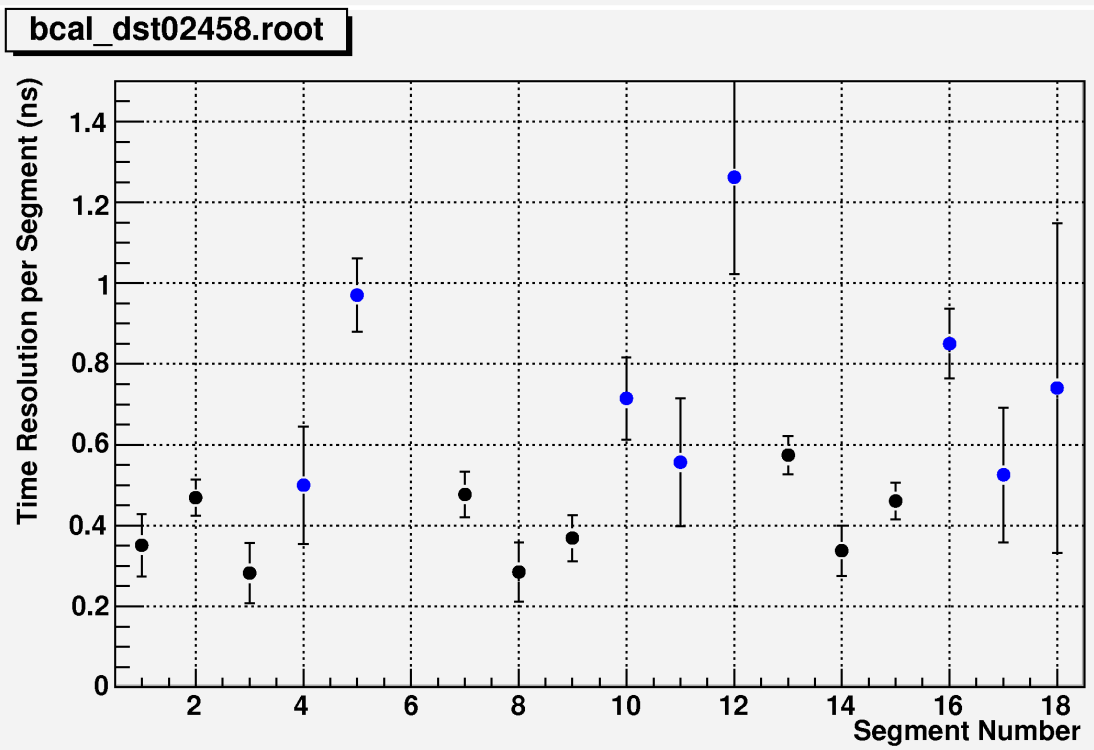

Figure 9: Summary of time resolutions of each segment from run 2458. Black symbols correspond to segments that read out with Philips XP2020 PMTs; blue symbols correspond to segments that read out with Burle 8575 PMTs.

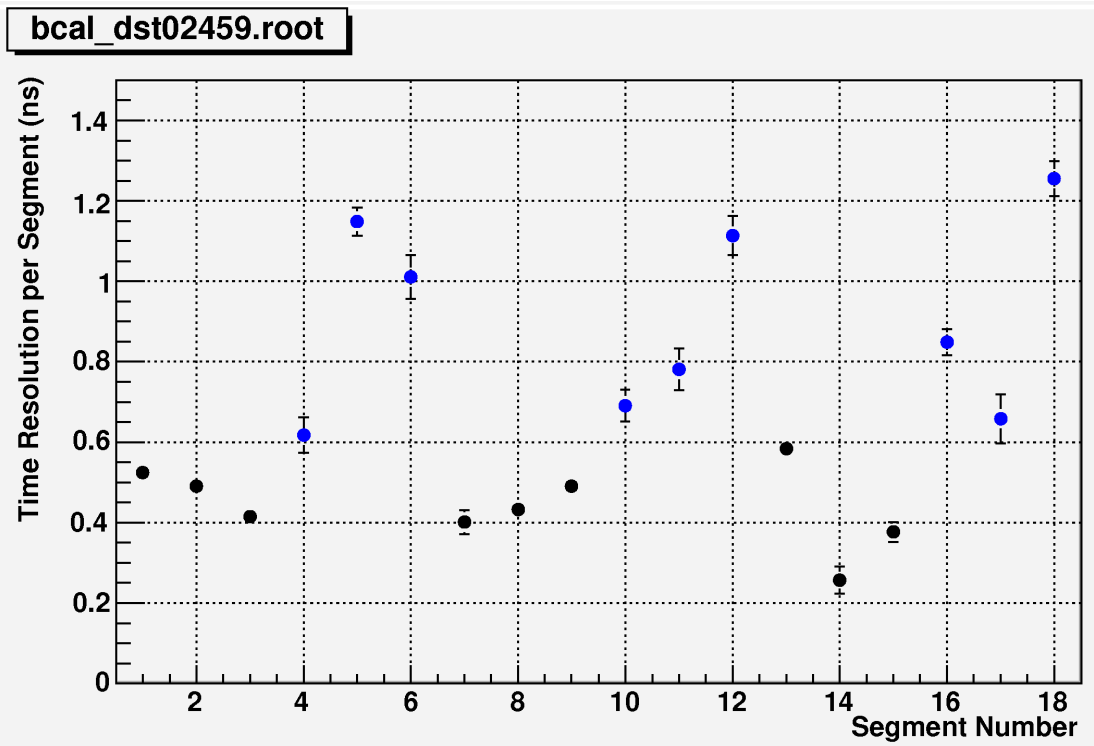

Figure 10: Summary of time resolutions of each segment from run 2459. Black symbols correspond to segments that read out with Philips XP2020 PMTs; blue symbols correspond to segments that read out with Burle 8575 PMTs.

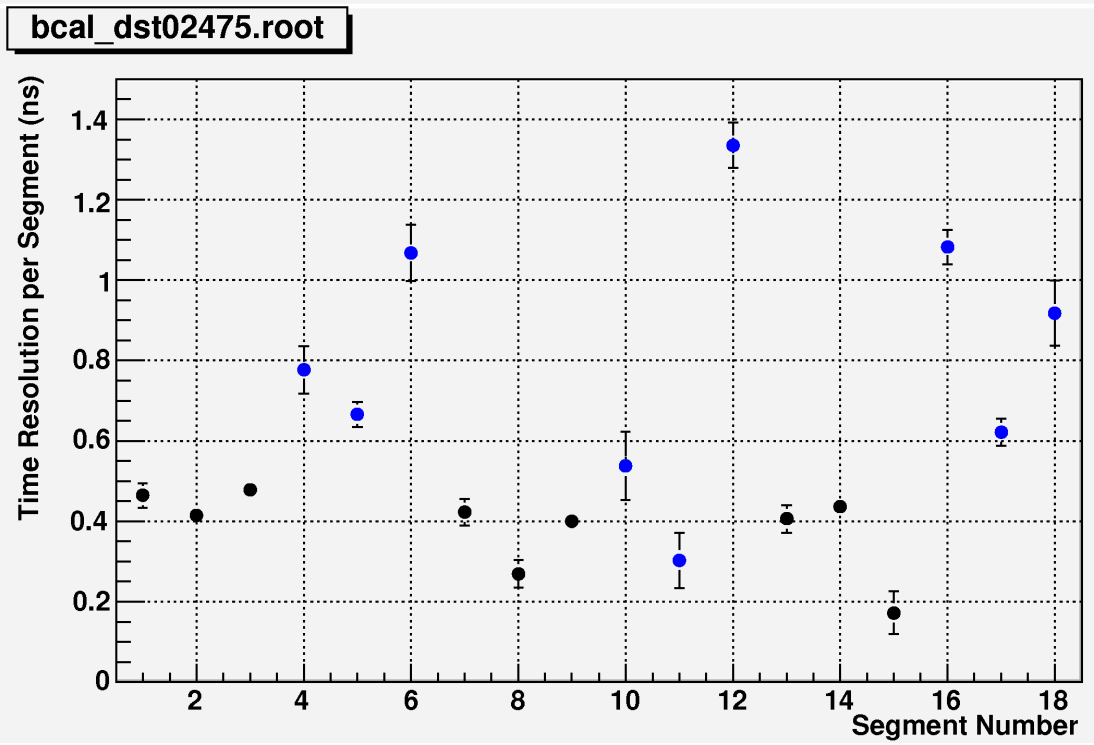

Figure 11: Summary of time resolutions of each segment from run 2475. Black symbols correspond to segments that read out with Philips XP2020 PMTs; blue symbols correspond to segments that read out with Burle 8575 PMTs.

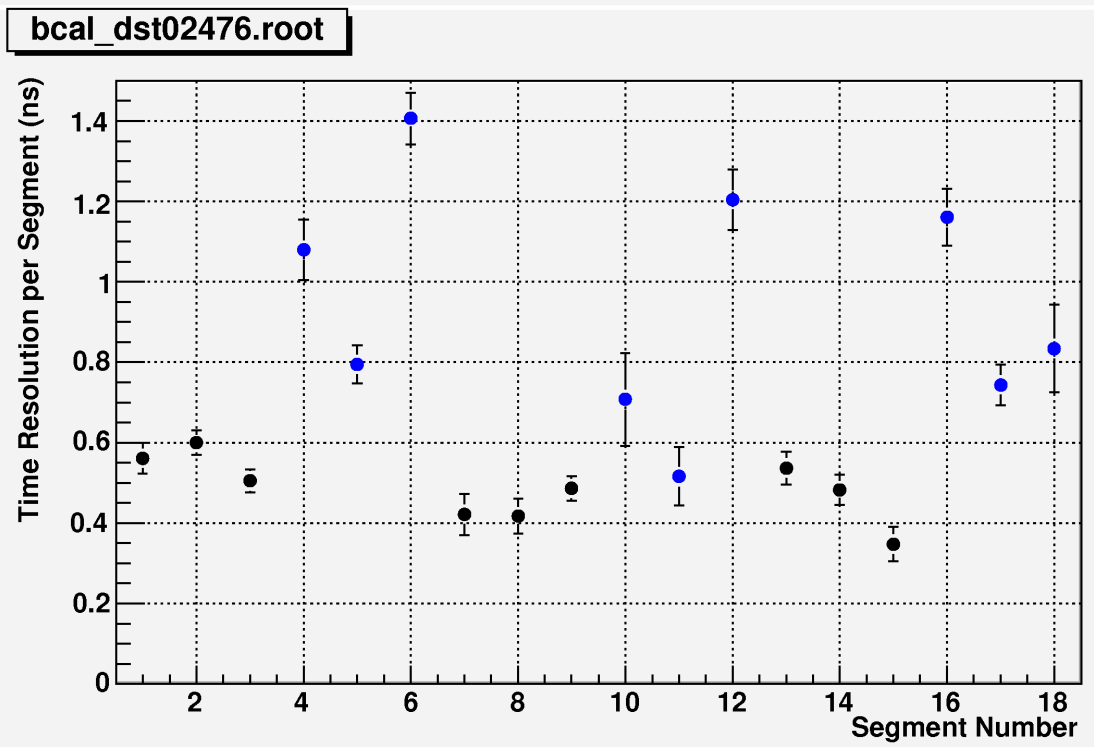

Figure 12: Summary of time resolutions of each segment from run 2476. Black symbols correspond to segments that read out with Philips XP2020 PMTs; blue symbols correspond to segments that read out with Burle 8575 PMTs.

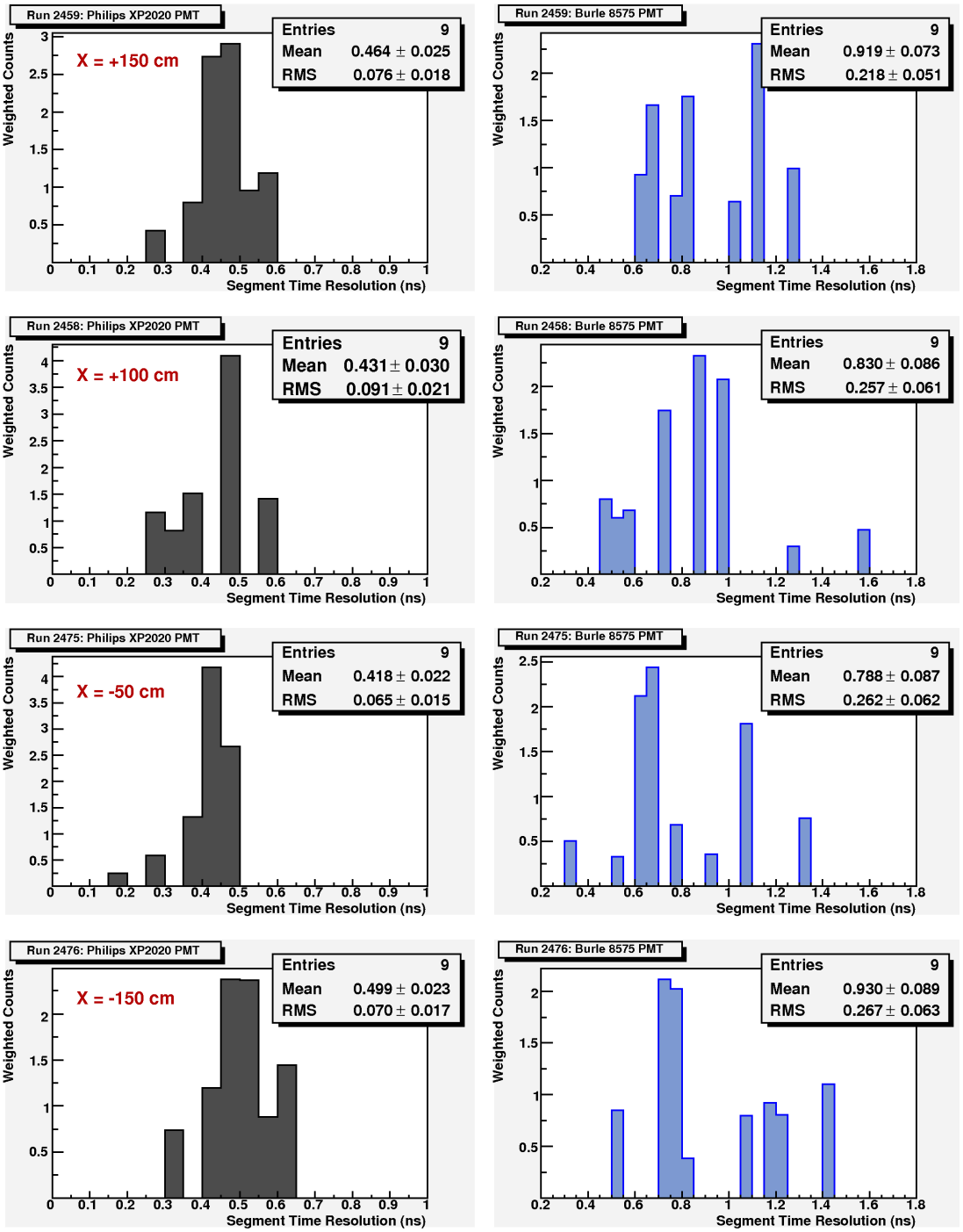

Figure 13: Distributions of segment time resolutions weighted on the uncertainty of segment time resolution measurement. Histograms in the left column correspond to segments that read out with Philips XP2020 PMTs; histograms in the right column correspond to segments that read out with Burle 8575 PMTs.

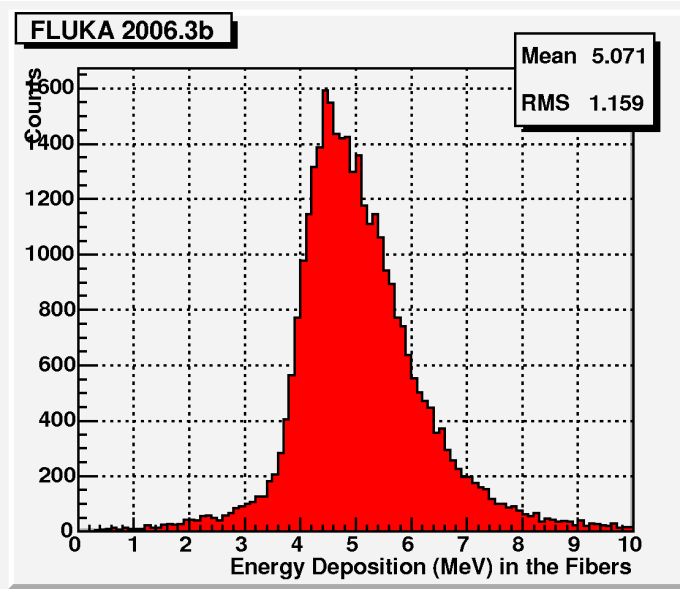

Figure 14: Typical spectra of energy deposited in the calorimeter segments by 5 GeV/c muons after muon" selection cuts were applied. (Result of the simulation with FLUKA 2006.3b program.)

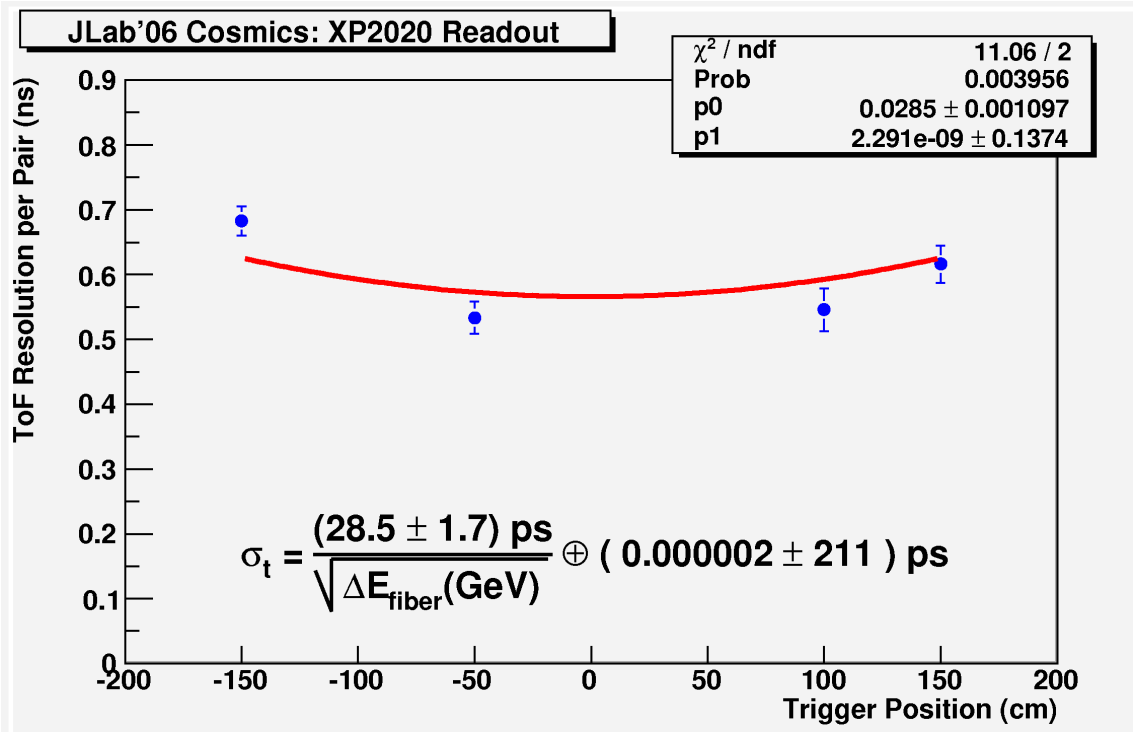

Figure 15: Fit the time resolutions of the pair of segments (averaged over the segments that were read out with Philips XP2020 PMTs) from thr four runs to the function (5).